Paper

A New Implementation of UWB CRLH Based Antennas for Wireless Communications

Mohammad Alibakhshi-Kenari and Mohammad Naser-Mogaddasi

Faculty of Engineering, Science and Research Branch, Islamic Azad University, Tehran, Iran

Abstract—In this article, a novel ultra wideband (UWB) small antennas based on the composite right/left-handed transmission lines structures are proposed. The antennas are presented with best in size, bandwidth and radiation patterns. Their physical size and the operational frequency depend on the unit cell size and the equivalent transmission line model parameters of the CRLH-TL. To realize characteristics of first proposed model, Q-shaped gaps printed into rectangular radiation patches are used. The antenna based on composite right/left-handed transmission lines is composed of two unit cells, each of which occupies only 10.8 × 8.6 mm and covers the 2.7–9.3 GHz bandwidth for VSWR < 2. The peak gain and radiation efficiency, are 5.78 dBi and 42.1% 9.3 GHz, respectively. Moreover, the second designed antenna has the same size and enhancement bandwidth, gain and radiation efficiency than the first proposed antenna with similar design procedure. It is constructed of the printed Q-shaped four unit cells. The length, width and height are 21.6, 8.6 and 1.6 mm, respectively, and it covers 4.1–11.7 GHz bandwidth for VSWR < 2 having highest gain (7.18 dBi) and radiation efficiency (92.69%) at 4.1 GHz.

Keywords—composite right/left-handed transmission lines, metamaterial, modern wireless communication systems, portable devices, printed Q-shaped antennas, small antennas, ultra wideband antennas.

1. Introduction

Since their invention in 1960s, the microstrip patch antennas have found numerous applications for their simplicity in fabrication, compatibility with planar circuitry, low profile and planar structures, and unidirectional radiation capability. Despite of its many electrical and mechanical features, their use at low frequencies has been limited due to limited size and narrow bandwidth.

The conventional approach for miniaturizing the antenna size is to print the radiator on a high-k dielectric substrate. However, because of the capacitive nature of the patch geometry and the existence of high impedance contrast between the antenna substrate and the free space surrounding region, a high energy is trapped inside the dielectric material resulting in a narrow bandwidth and high radiation loss.

The metamaterials (MTMs) are very attractive for the design of small antennas and microwave devices [1], [2]. The composite right/left handed transmission lines (CRLH-TLs) provides a conceptual route for implementing small antennas. CRLH-based antennas can also be made broadband to support today's multi band communication and wireless applications requirements. The commercial uses of frequency band 3 to 10.6 GHz for radar, tracing, and data transmissions were approved by FCC in 2002 [3]. Recently, the research and development of the UWB communication systems including antennas have been widely performed [4]–[6]. One of the main port of the UWB system is an antenna providing low (< 2) VSWR over 3–10.6 GHz band. The designed two CRLH-based antennas support all cellular frequency bands (from 2.7 to 11.7 GHz), using single or multiple feed, which eliminates switches. Significant size reduction is also demanded to achieve the minimization of communication systems or devices. Ideally, the UWB antenna should be small, planar, then low cost and reliable. Also, compatibility and ease of integration with electronics for mobile communications are desirable. Furthermore, in order to satisfy the various demands for communication and wireless services, small antenna with wide bandwidth and good radiation characteristics are needed. Two designed antennas are based on CRLH-TLs, which results of very wideband and good radiation properties.

Developments of wireless communications systems call for more compact and multi band antennas to coexist in a small area, while maintaining their low coupling to support multipath channel decorrelation. Metamaterial structures have the ability to concentrate electromagnetic fields and currents near antenna structures, instead of spreading them along the ground, causing higher coupling. This allows compact antenna arrays to be realized with minimal mutual coupling, to be able to decorrelate multipath channels in MIMO implementations [7]–[8]. In this paper, the authors will focus on transmission lines (TL) based on composite right- and left-hand (CRLH) propagation [9]–[24]. It is nearly impossible to implement a pure left-handed (LH) transmission line due to the right-handed (RH) propagation inherited by using lumped elements [9]. Such transmission lines make possible unprecedented improvements in air-interface integration, over-the-air (OTA) functionality and miniaturization, while simultaneously reducing bill-of-materials costs and specific absorption rate (SAR) values. Metamaterials enable physically small but electrically large

air-interface components, with minimal coupling among closely spaced devices.

Metamaterials (MTM) are manmade composite materials, engineered to produce desired electromagnetic propagation behavior not found in natural media [9]–[10]. The word metamaterial refers to their many variations. Metamaterial antenna structures are copper, printed directly on the dielectric substrate, and can be fabricated by using a conventional Rogers RT Duroid 5880 substrate or a flexible printed circuit (FPC) board. Recently, a novel antennas with these characteristics have been designed by using CRLH-TL metamaterials [11]–[12]. Unlike traditional RH transmission materials, metamaterials based on LH transmission lines have unique features of anti-parallel phase and group velocities ($v_p - \|v_g$) [11]–[13]. Pure LH TLs cannot be implemented due to the existence of RH parasitic effects that occur naturally in practical LH TLs. CRLH-TL structures have been proposed, which also include RH effects. Several metamaterials-based antennas have already been presented, such as backward-to-forward leaky-wave [14]–[15], zeroth-order resonant [16], and so on.

Metamaterials are broadly defined as effectively homogeneous artificial structures exhibiting unusual properties, e.g. theirs index of refraction that may be negative (left handedness), less than one, or modulated in a graded manner. Such materials have spurred considerable interest and led to numerous applications over the past decade [18]–[19].

Metamaterials may be equivalently described in terms of media parameters (electric/magnetic dipole moments, electric/magnetic susceptibilities, permittivity, permeability), or in terms of transmission line parameters (inductance, capacitance, impedance, admittance, propagation constant, characteristic impedance). The latter approach, introduced in [20]–[21], has led to low-loss and broadband metamaterials, due to the non-resonant nature of the structural elements. This has been the foundation for the vast majority of the practical applications reported to date. More particularly, the concept of CRLH transmission line metamaterials, which describes in a simple and insightful manner the fundamentally dual RH/LH nature of metamaterials, has been widely recognized as a powerful paradigm for the understanding of metamaterial phenomena and the design of metamaterial devices [22], [23].

The applications of metamaterials may be classified in three categories:

- guided-wave components: multi-band, enhanced bandwidth, and miniaturized components, tight broadband couplers, compact resonators, uniform power combiners and splitters, UWB filters, agile distributed amplifiers, impulse delay lines and circuits;

- refracted-wave systems: focusing slabs, super-resolution imagers, reflection-less curved refractors, coordinate-transformation-based graded-index structures for electromagnetic manipulations;

- radiated-wave devices: mono/multi band passive/active one dimensional/two dimensional printed planar antennas and reflectors.

This article is concerned with the third category. It presents a selected number of the most practical CRLH metamaterial printed planar antennas based on utilizing CRLH metamaterial transmission lines technology and printed planar methodology, which have enhancement bandwidth and radiation characteristics.

The paper is organized as follows. Section 2 introduced antenna based on composite right/left-handed metamaterial transmission lines. Section 3 recommends a new idea of the design UWB small CRLH MTM antennas. In Section 4 the simulation results and discussions of the proposed printed antennas arrangements are presented. Afterwards in Section 5 provides a brief talk about benefits of the presented CRLH based antennas. Finally, discussion and conclusion are raised in Section 6.

2. Antennas Based on Composite Right/Left-Handed Metamaterial Transmission Lines

2.1. Fundamentals of CRLH Metamaterial TL Structures

Figure 1 shows the equivalent circuit of periodic CRLH metamaterial transmission lines (MTM TLs) in general case (lossy case). It should be noted that periodicity is here a convenience but not a necessity, as long as the largest cell is much smaller than the guided wavelength ($p \ll \lambda_g$) for electromagnetic homogeneity. Another important note is that as long as the effective medium condition, $p \ll \lambda_g$ is satisfied, there is no constraint on the minimum number of unit cells required for metamaterial operation. Even one single cell, when perfectly matched to the external world (i.e., presenting a block impedance equal to that of the external media or ports), behaves in a manner that cannot be distinguished from the behavior of a perfectly continuous medium of the same electrical size for the wave crossing it.

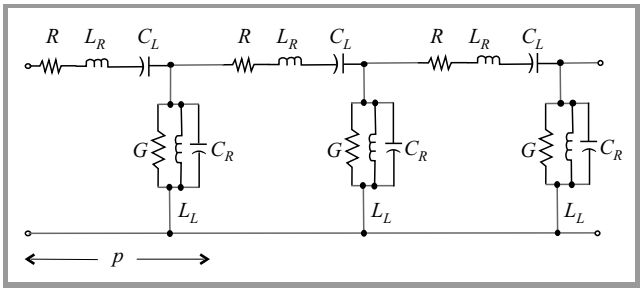

Fig. 1. The equivalent circuit model of periodic homogeneous CRLH metamaterial transmission lines structures composed of P unit cells in general case.

The homogeneous models of RH, LH, and CRLH lossless transmission lines are shown in Fig. 2 [11]. For a RH

lossless TL, its model is developed from conventional infinitesimal circuit model, where L_R is a series inductance and C_R is a shunt capacitance. The LH model is obtained by interchanging the inductance/capacitance and inverting the series/parallel arrangements in the equivalent circuit of the RH-TL, where C_L presents a series capacitance and L_L presents a shunt inductance. In effect, parasitic capacitance C_R due to development of voltage gradients and unavoidable parasitic inductance L_R due to current flow along the metallization will be added to LH TL and result in CRLH TL structure [11].

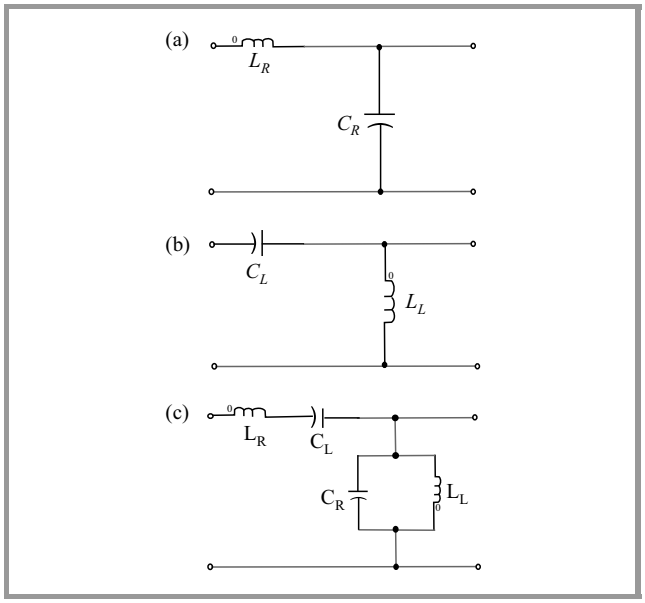

Fig. 2. Equivalent homogenous circuit models: (a) RH TL, (b) LH TL, (c) CRLH TL.

The model values R, L, C, G are known as the primary line parameters, from which the secondary line values are derived. The propagation constant value γ, for a given system is defined by the amplitude at the source of the wave to the amplitude at distance x, and [28] expressed as:

$$\frac{A_0}{A_x} = e^{\gamma x}. \tag{1}$$

Note that γ is a complex form:

$$\gamma = \alpha + j\beta, \tag{2}$$

where α is the real part called the attenuation and β, the imaginary part, is called the phase.
For example in a copper transmission line, the propagation constant can be calculated from the primary line constants by means of the relationship:

$$\gamma = \sqrt{ZY}, \tag{3}$$

where Z and Y are the impedance and admittance of the transmission line. In the special case of the CRLH TL, Z and Y are defined as [11]:

$$Z(\omega) = j\left(\omega L_R - \frac{1}{\omega C_L}\right), \tag{4}$$

$$Y(\omega) = j\left(\omega C_R - \frac{1}{\omega L_L}\right). \tag{5}$$

The dispersion relation for a homogenous CRLH TL is [11]:

$$\beta(\omega) = s(\omega)\sqrt{\omega^2 L_R C_R + \frac{1}{\omega^2 L_L C_L} - \left(\frac{L_R}{L_L} + \frac{C_R}{C_L}\right)}, \tag{6}$$

where

$$s(\omega) = \begin{cases} -1 & \text{if } \omega < \omega_{se} = \min\left(\frac{1}{\sqrt{L_R C_L}}, \frac{1}{\sqrt{L_L C_R}}\right) \\ 0 & \text{if } \omega_{se} < \omega < \omega_{sh} \\ +1 & \text{if } \omega < \omega_{sh} = \max\left(\frac{1}{\sqrt{L_R C_L}}, \frac{1}{\sqrt{L_L C_R}}\right) \end{cases}. \tag{7}$$

Figure 3 shows the ω-β or dispersion diagram of a RH TL, LH TL, and CRLH TL, respectively. The group velocity or $v_g = \frac{\partial\omega}{\partial\beta}$ slope and phase velocity or the line segment slope from origin to curve ($v_p = \frac{\omega}{\beta}$) of these TLs can be inferred from the dispersion diagram. For a purely RH TL, it is shown that v_g and v_p are in parallel ($v_g \| v_p$ and $v_g v_p > 0$).

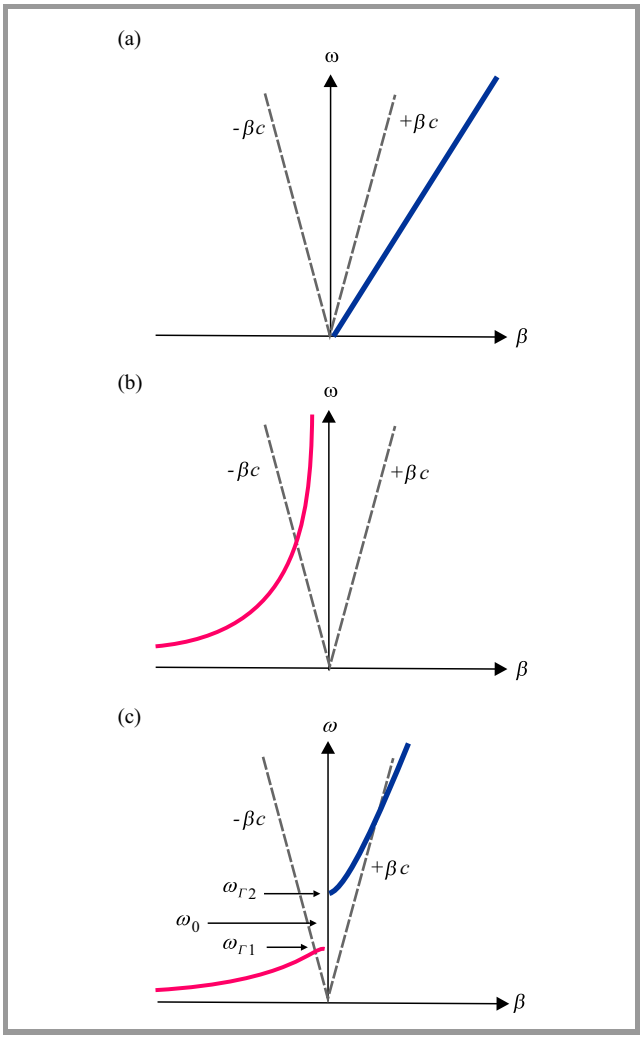

Fig. 3. Dispersion diagrams for homogenous: (a) RH TL, (b) LH TL, (c) CRLH TL (unbalanced case).

However, for a purely LH TL, the negative sign in $\beta(\omega)$ indicates a negative phase velocity and therefore v_p and v_g are anti-parallel ($v_p - \| v_g$ and $v_p v_g < 0$). In addition, Fig. 3 shows that, it has both LH ($v_p v_g < 0$) and RH ($v_p v_g > 0$) region. Also note that the stop band occurs in the frequency range where γ is purely real for a CRLH TL ($\beta = 0$). The group and phase velocities of the transmission line can be defined as:

$$v_g = \left(\frac{\partial \beta}{\partial \omega}\right)^{-1} = s\omega^2 \sqrt{L_L C_L}\,, \tag{8}$$

$$v_p = \frac{\omega}{\beta} = s\omega^2 \sqrt{L_L C_L}\,, \tag{9}$$

where s is a sign function defined as:

$$s = \left\{ \begin{array}{ll} +1 & \text{for RH TL} \\ -1 & \text{for LH TL} \end{array} \right\}. \tag{10}$$

LH-TL ihas high-pass nature, in contrast to that of the RH-TL which is of low-pass nature, in result a CRLH-TL contributes LH property at lower frequencies and RH at higher frequencies with a transition frequency ω_0. When the series and shunt resonances (ω_{se} and ω_{sh}) are equal, i.e.:

$$\omega_{se} = \frac{1}{\sqrt{L_R C_L}} = \omega_{sh} = \frac{1}{\sqrt{L_L C_R}} \tag{11}$$

or

$$L_R C_L = L_L C_R\,, \tag{12}$$

the propagation constant in Eq. (6) reduces to the simpler expression [11]

$$\beta = \beta_R + \beta_L = \omega\sqrt{L_R C_R} - \frac{1}{\omega\sqrt{L_L C_L}}\,, \tag{13}$$

where the phase constants splits up into β_R and β_L. Thus, there is a seamless transition from LH to RH for the balanced case occurring at the transition frequency ω_0 [11]:

$$\omega_0^{\text{unbalanced}} = \frac{1}{\sqrt[4]{L_R C_R L_L C_L}} \tag{14}$$

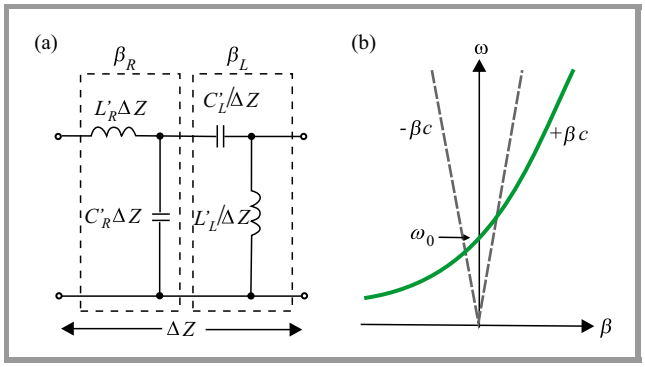

Fig. 4. Balanced form of: (a) simplified equivalent circuit model, (b) dispersion diagram showing seamless transition from LH to RH region.

and in the balanced case, $\omega_0^{\text{balanced}}$ is:

$$\omega_0^{\text{balanced}} = \frac{1}{\sqrt{L_R C_L}} = \frac{1}{L_L C_R}\,. \tag{15}$$

A balanced form of a CRLH TL is shown in Fig. 4. The simplified equivalent circuit model is the series combination of RH and LH TLs. Also, the balanced CRLH TL's dispersion curve does not have a stop band. At ω_0 the phase shift ($\varphi = -\beta d$) for a TL of length d is zero ($\beta = 0$). Phase advance ($\varphi > 0$) occurs in the LH frequency range ($\omega < \omega_0$, $\beta < 0$), and phase delay ($\varphi < 0$) occurs in the RH frequency range ($\omega > \omega_0$, $\beta > 0$) [11].

The TL characteristic impedance is $Z_0 = \sqrt{\frac{Z}{\gamma}}$. In unbalanced case:

$$Z_0 = Z_L \sqrt{\frac{C_L L_R \omega^2 - 1}{C_R L_L \omega^2 - 1}} \tag{16}$$

in the balanced case: $Z_0 = Z_L = Z_R$, and

$$Z_L = \sqrt{\frac{L_L}{C_L}} \tag{17}$$

$$Z_R = \sqrt{\frac{L_R}{C_R}}\,, \tag{18}$$

where Z_L and Z_R are the purely LH and RH impedances, respectively. According to Eq. (16) the characteristic impedance for the unbalanced case is frequency dependent, however, according to Eqs. (17) and (18) for the balanced case is frequency independent and therefore, can be matched over a wide bandwidth.

The TL material permeability and permittivity have been related to the impedance and admittance of its equivalent TL model:

$$\mu = \frac{Z}{j\omega} = L_R - \frac{1}{\omega^2 C_L}\,, \tag{19}$$

$$\varepsilon = \frac{Y}{j\omega} = C_R - \frac{1}{\omega^2 L_L}\,. \tag{20}$$

Equations (19) and (20) prove that for balanced case the permeability and permittivity are negative in LH region ($\omega < \omega_0$).

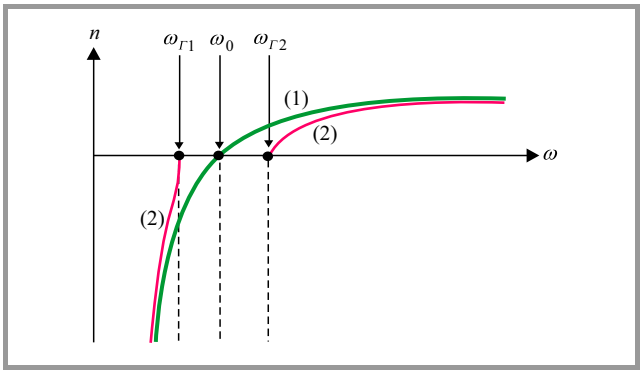

Fig. 5. Typical refraction index plots for the balanced (1) and unbalanced (2) CRLH TL.

The refraction index ($n = \frac{c\beta}{\omega}$) for the balanced and unbalanced CRLH-TL is shown in Fig. 5 [11]. As depicted

the CRLH-TL has a negative refraction index in its LH range and a positive refraction index in its RH range.

2.2. CRLH Metamaterials in Antenna Design

The antenna has become one of the most important component when designing wireless communication systems in portable devices. Due to the limited space available, shrinking conventional antennas may lead to performance degradation and complicated mechanical assembly. Metamaterial technology provides an opportunity to design of a smaller size antenna at lower cost with better radiation performance. Various implementations of metamaterial structures have been reported and demonstrated in [9]–[10]. In this article, a transmission line type of realization CRLH-TL that possesses characteristics of low insertion loss, broad bandwidth, low profile and good radiation performance will be employed.

A metamaterial is usually a periodic structure with N identical unit cells cascading together, where each cell is much smaller than one wavelength at the operational frequency. The composition of one metamaterial unit cell is categorized as a series inductor (L_R) and capacitor (C_L), shunt inductor (L_L) and capacitor (C_R). L_L and C_L determine the left-handed mode propagation properties, while L_R and C_R govern the right-handed mode propagation properties. The behavior of both propagation modes at different frequencies can be easily addressed in a simple dispersion diagram, as shown in Fig. 6. The dispersion curve on the $\beta > 0$ side

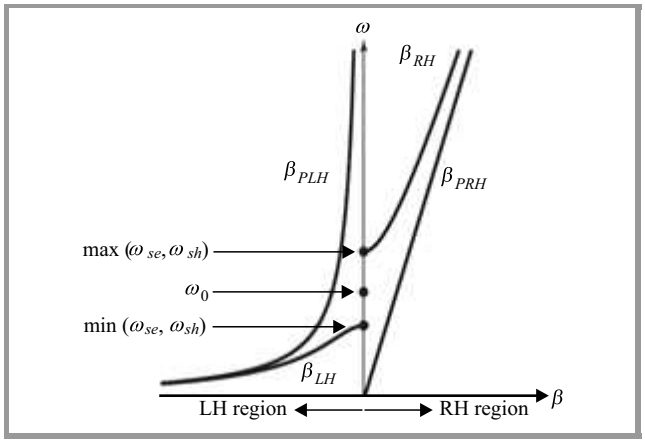

Fig. 6. Dispersion diagrams for a CRLH TL (unbalanced case).

is the right-handed mode, while the dispersion curve on the $\beta < 0$ side is the left-handed mode [9]. The electrical size of a conventional transmission line is strongly related to its physical dimensions and thus reducing device size usually means increasing operational frequency. In contrary, the dispersion curve of a metamaterial is determined by the four CRLH parameters. If these four parameters are realized in a very compact form, the corresponding circuit size will be physically small but electrically large. This concept has been adopted successfully in small antenna designs [7]–[25].

3. UWB and Small CRLH MTM Antenna Design

3.1. Printed Q-Shaped Two Unit Cells Antenna

The equivalent circuit model design of the proposed MTM antenna is based on the CRLH-TL structure shown in Fig. 7. The proposed planar antenna is fabricated on an Rogers RT

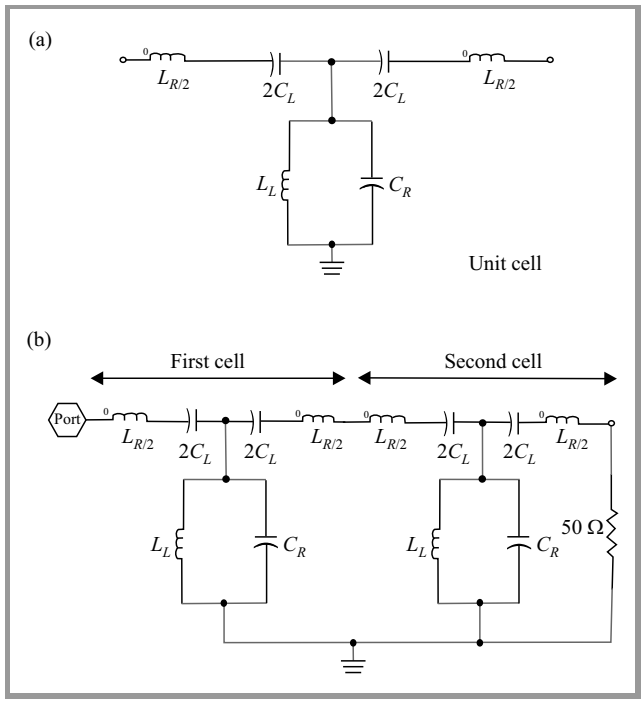

Fig. 7. The equivalent circuit model of the proposed printed Q-shaped antenna: (a) unit cell, (b) whole structure.

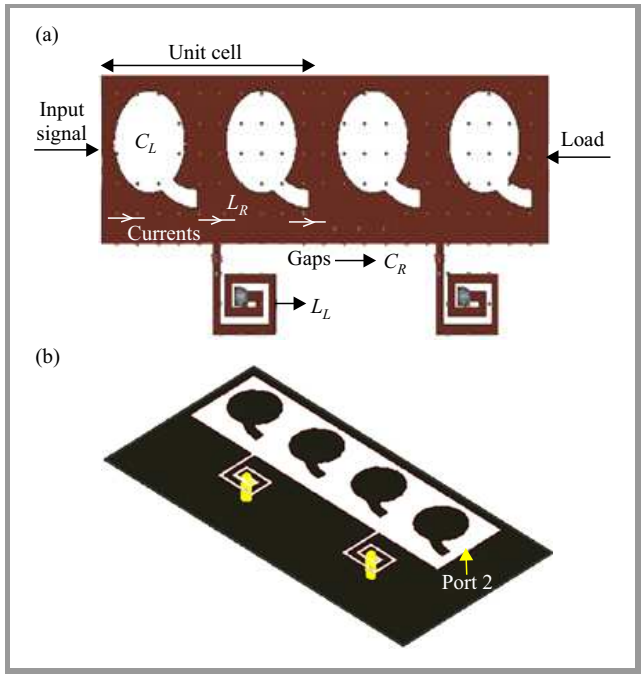

Fig. 8. Proposed printed Q-shaped antenna: (a) top view, (b) 3D view.

Duroid 5880 substrate, with a 2.2 dielectric constant, and a thickness of 1.6 mm. This mushroom type unit cell consisted of a 10.8 × 8.6 mm top patch, printed on top of the substrate and a rectangular inductor attending a metallic via. Each unit cell was coupled to its adjacent unit cell and the vertical via was connected between the rectangular inductor and the ground on the back of the substrate. This antenna was excited by external port as input signal, as shown in Fig. 8. The shape and dimensions were optimized for matching purposes, reducing of the occupy area, enhancement bandwidth and providing good radiation properties.

The antenna is based on two simplified planar mushroom structure unit cells. The unit cell is composed of a host transmission line with two printed Q-shaped gaps into rectangular radiation patches and a rectangular inductor connected to ground plane through a metallic via. The Q-shaped gaps printed within patches operates as series capacitance (C_L) and the rectangular inductor accompanying vertical metallic via hole connected to ground plane performs a shunt inductance (L_L). A purely left-handed transmission line cannot exist physically because, of parasiting effects increasing with frequency. Thus, the CRLH model represents the most general MTM structure possible. This antenna structure is excited by external port (Port 1) as input signal and Port 2 is matched to 50 Ω load impedance of the SMD 1206 size components connected to ground plane through a via. Configuration of the proposed printed Q-shaped two unit cells antenna is shown in Fig. 8.

Presented antenna is formed of the two simplified planar mushroom structure Q-shaped unit cells, each of which occupies only 10.8 × 8.6 mm or $0.18\lambda_0 \times 0.15\lambda_0$ at the resonance frequency $f = 5.2$ GHz, therefore, the physical dimensions are 21.6, 8.6 and 1.6.

The important issue of many conventional metamaterial antennas confront is a lack of bandwidth [26]–[27].

The transmission coefficient is an important frequency domain performance indicator of an UWB antenna [29]. In this paper, the authors proposed several method to extend the bandwidth of the MTM antennas with a fixed antenna size. The points summarize in below, are guidelines for such design:

- traveling wave antennas or antennas having low Q can be very broadband [37];
- antennas incorporating tapers or rounded edges tend to give broad bandwidths because surface currents have a smooth path to follow [30];
- linearly polarized antennas are the simplest to implement in a compact planar package;
- minimizing the thickness of the substrate and using low loss materials maximizes radiation efficiency [40];
- using of the printed planar technology into radiation patches for antenna design with minimizing acceptable distance between gap edges results to extended the bandwidth of the antenna [38]–[39].

In this article, the 2, 4 and 5 approaches for increasing the bandwidth are used. By using a smaller value of the loaded C_L on the CRLH-TL, broadband performance can be obtained. A smaller value of the loaded C_L will be realized by implementation of the Q-shaped gaps with closely space edges printed into rectangular patches. This method is used to increase the bandwidth, as providing UWB antenna with 6.6 GHz bandwidth (from 2.7 GHz to 9.3 GHz) for VSWR < 2. The antenna gain and radiation efficiency at resonance frequency $f_r = 5.2$ GHz are equal to 4.71 dBi and 41.82%, respectively. The simulated reflection coefficient ($S_{11} < -10$ dB) and radiation gain pattern at $f_r = 5.2$ GHz are plotted in Figs. 9 and 10, respectively.

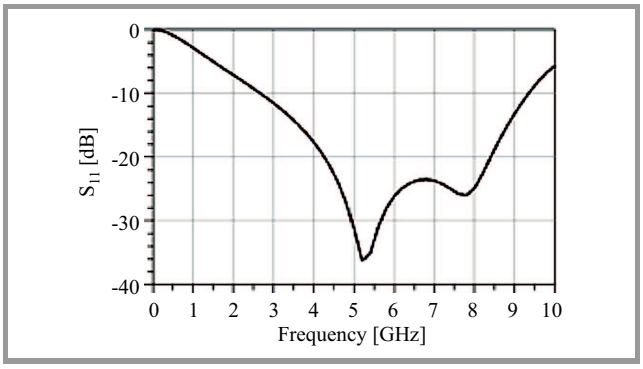

Fig. 9. Simulated reflection coefficient.

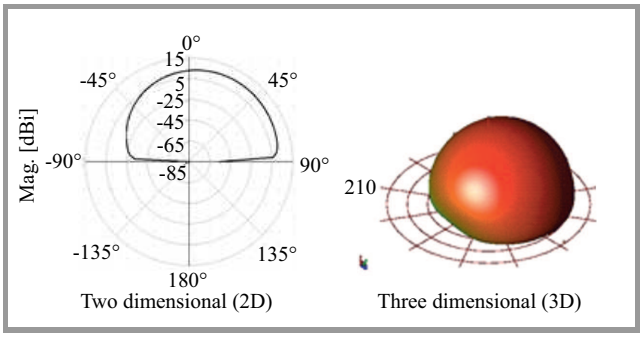

Fig. 10. The radiation gain pattern in elevation plane ($\Phi = 0°$) and at resonance frequency $f_r = 5.2$ GHz.

Next, an useful MTM antenna based on two simplified planar mushroom structure unit cells is designed. Its configuration employing the proposed methods is shown in Fig. 8. The performance of the presented designing methods and antenna structure are verified using Agilent ADS full-wave simulator.

3.2. Improvement Gain Antenna with Printed Q-Shaped Four Unit Cells Structure

In this section, the four unit cells printed Q-shaped antenna structure with enhancement bandwidth, radiation gain and efficiency in comparison structure proposed in previous section. The design procedure is completely same,

but equivalent circuit model and geometry is different. Presented antenna in this section is designed as one rectangular inductor attending a via are considered for each gap area which become one constructing one unit cell, in results this antenna composed of four unit cells as shown in Fig. 12. Equivalent circuit model is shown in Fig. 11. As obvious recent structure composed of four unit cells as each unit cell consist of a series capacitance (C_L) which created by printed Q-shaped gap capacitance, a shunt inductance (L_L) that caused with a rectangular inductor connected to ground plane through a via as these capacitor an inductor plays left-handed roles, also a series inductance (L_R) which established by unavoidable current flow on the patches and a shunt capacitance (C_R) that performed with gap capacitor between patches and ground plane.

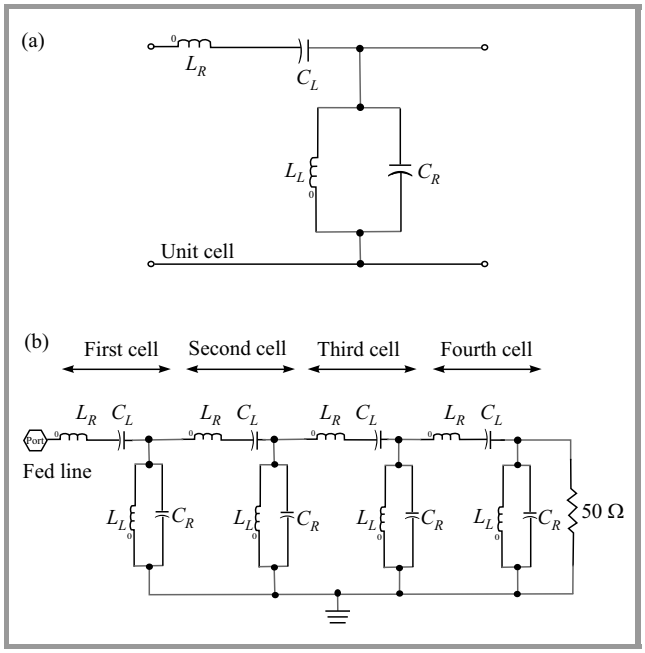

Fig. 11. The equivalent circuit model of four unit cells printed Q-shaped antenna: (a) unit cell, (b) whole structure.

This typical CRLH antenna structure consists of a feed line that is electromagnetically coupled to metallic patches, rectangular inductors, via that connects the rectangular inductor to the ground plane. This feed line through a small gap excites the CRLH unit cells. Typically, the antenna is matched to a port with 50 Ω load impedance. The resonant frequency, matching of multiple right-handed and left-handed modes, and associated efficiencies can be controlled by the size of the cell patch, the via line width, the feed line length, the distance between the antenna elements and the ground, optimizing the rectangular inductor and various other dimensions and layouts [7]–[17]. The gap capacitor and the rectangular inductor accompanying a via could be viewed as C_L and L_L, while the top patch possessed the L_R and C_R to the ground. Therefore, a left-handed resonance could be obtained at the desired frequency by properly designing the gap capacitor and the rectangular inductor that connected to ground plane through a via. Formation of the recommended antenna with enhancement bandwidth and improvement radiation properties is shown in Fig. 12.

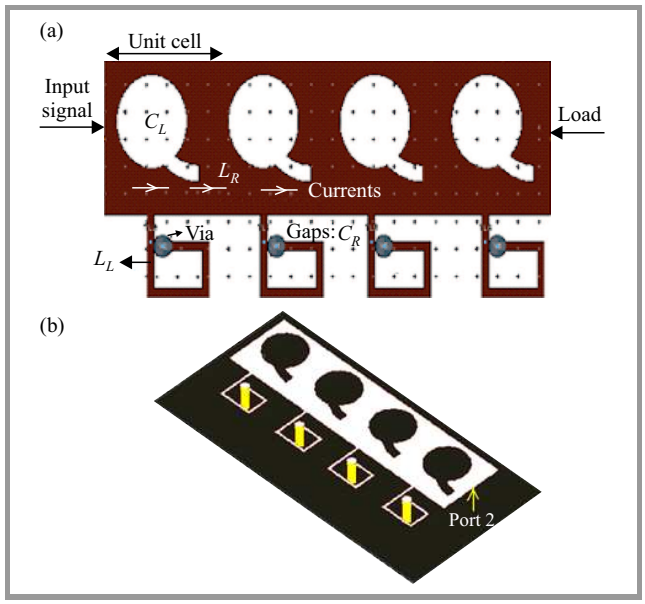

Fig. 12. Formation of the four unit cells printed Q-shaped antenna: (a) top view, (b) isometric view.

Printed Q-shaped antenna was designed on Rogers RT Duroid 5880 substrate with dielectric constant $\varepsilon_r = 2.2$ and thickness $h = 1.6$ mm. It is formed of the four simplified planar mushroom structure Q-shaped unit cells, each of which occupies 5.4×8.6 mm or $0.1\lambda_0 \times 0.16\lambda_0$ at the resonance frequency $f_r = 5.65$ GHz, where λ_0 is free space wavelength, therefore overall size of the Q-shaped antenna is $21.6 \times 8.6 \times 1.6$ mm^3 ($0.4\lambda_0 \times 0.16\lambda_0 \times 0.03\lambda_0$). This antenna has 7.6 GHz applicable bandwidth from 4.1 to 11.7 GHz for VSWR < 2, which corresponds to 96.2% practical bandwidth. In addition at resonance frequency $f_r = 5.65$ GHz the gain and radiation efficiency are 6.52 dBi and 60.47%, respectively. The simulated return loss bandwidth (S_{11}) of the antenna and radiation gain pattern at $f_r = 5.65$ GHz are plotted in Figs. 13 and 14 respec-

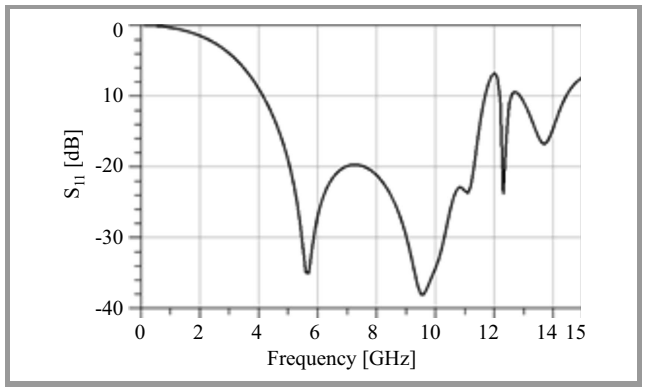

Fig. 13. Simulated return loss (S_{11}).

tively. The results show that with the same physical size, broader bandwidth and superior radiation performances was achieved.

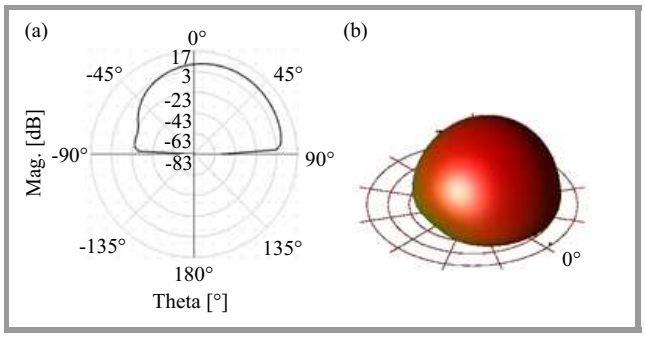

Fig. 14. The radiation gain pattern in elevation plane ($\Phi = 0^\circ$) and at resonance frequency $f_r = 5.65$ GHz: (a) 2D view, (b) 3D view.

Entire equivalent circuit model and configuration of the both Q-shaped antennas are illustrated in Fig. 7. Two designed UWB small antennas based on CRLH MTM-TLs are suitable and useful for microwave and portable devises and wireless communication applications.

4. Simulation Results and Discussion of the Proposed Printed Antennas

Figure 9 and Fig. 13 show the simulated return losses of the two unit and four unit cells obtained by using Agilent ADS full-wave simulator. The simulated return losses bandwidth ($S_{11} < -10$ dB) of the first presented antenna is 6.6 GHz (from 2.7 to 9.3 GHz), this corresponds to 110% practical impedance bandwidth, which is more than conventional. The simulated return losses bandwidth ($S_{11} < -10$ dB) of the second device (Fig. 13) is 7.6 GHz (from 4.1 to 11.7 GHz), which corresponds to 96.2% practical impedance bandwidth, which is more than conventional realizations. The simulated 2D radiation gain patterns of the recommended antennas at different frequency are plotted in Figs. 15 and 16. For first antenna,

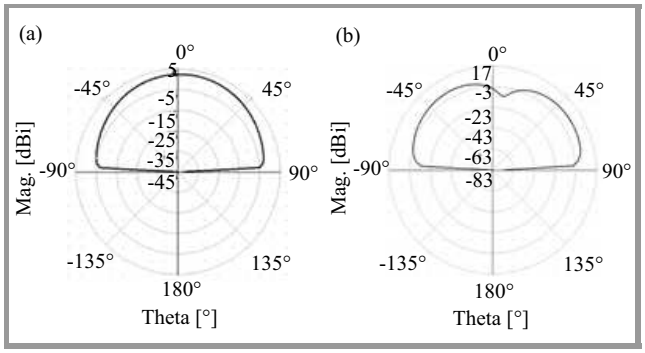

Fig. 15. The simulated radiation gain patterns of the two unit cells antenna in elevation plane ($\Phi = 0^\circ$): (a) at 47 GHz and (b) 9.3 GHz.

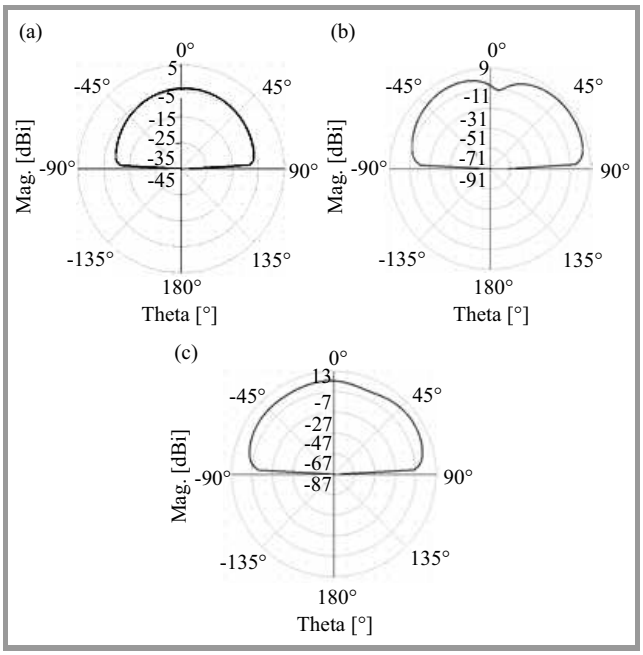

Fig. 16. The simulated radiation gain patterns of the 4-cells antenna in elevation plane ($\Phi = 0^\circ$) at three different frequencies.

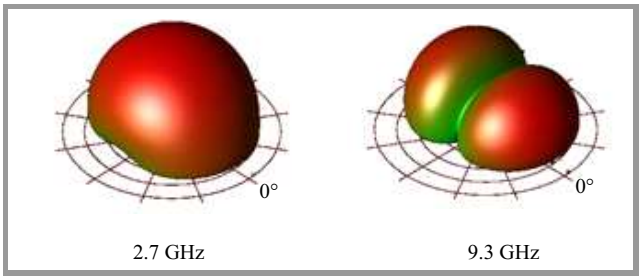

Fig. 17. Simulation of radiation gain patterns of the 2-cells antenna in elevation plane ($\Phi = 0^\circ$) at two frequencies.

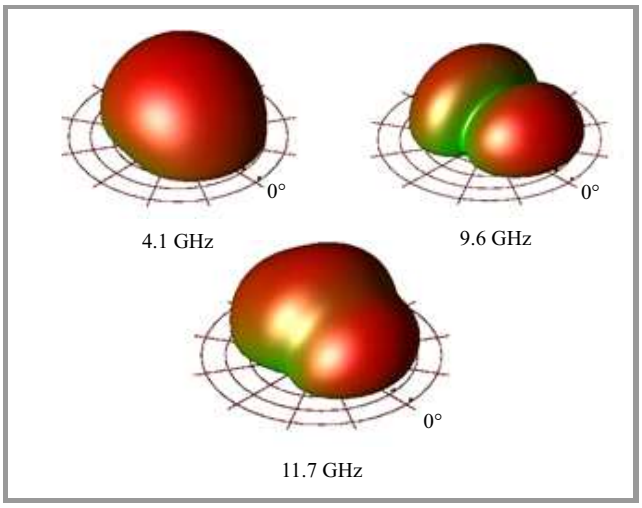

Fig. 18. Simulation of radiation gain patterns of the 4-cells antenna in elevation plane ($\Phi = 0^\circ$) at 3 frequencies.

radiation gains are 2.8 dBi and 5.78 dBi, respectively, at 2.7 and 9.3 GHz. Also, radiation efficiencies are 37.23 and 42.1% at same frequencies, respectively. For second

antenna, at 4.1, 9.6 and 11.7 GHz, gain and efficiency are 7.18 dBi and 92.69%, 5.83 dBi and 34.89%, and 5.42 dBi and 54.19%, respectively.

Table 1
Radiation characteristics of two typical antennas in comparison to the proposed

Parameters	Antenna described in [26]	Antenna described in [31]	Proposed first antenna	Proposed second antenna
Gain [dBi]	0.6	0.45	5.78	7.18
Bandwidth [GHz]	1–2	0.8–2.5	2.7–9.3	4.1–11.7
Efficiency [%]	26	53.6	42.1	92.69

Table 2
Comparison of dimensions of antennas

UWB antennas	Design size
Slotted planar binomial monopole antenna [32]	$30 \times 27.4 \times 1$ mm
Slotted circular monopole antenna [33]	$26 \times 27 \times 1$ mm
Slotted rectangular monopole antenna [34]	$18 \times 20 \times 1$ mm
Fork shaped antenna [35]	$35 \times 30 \times 0.769$ mm
Slotted arc shaped edge rectangular antenna [36]	$24 \times 35 \times 0.8$ mm
Both proposed UWB antennas	$21.6 \times 8.6 \times 1.6$ mm

According to Figs. 15 and 16 radiation patterns are unidirectional. The peak gain and radiation efficiency of the both versions occur at 9.3 and 4.1 GHz and are equal to 5.78 dBi and 42.1%, and 7.18 dBi and 92.69%, respectively. The simulated 3D radiation gain patterns at different frequencies are plotted in Figs. 17 and 18. To validate the design procedures the proposed antennas were compared with well-known compact UWB antennas and their characteristics were summarized in Tables 1 and 2.

5. CRLH-Based Antennas Benefits

The proposed CRLH-based antennas are wideband, low profile and compact in size, smaller than 50 by 10 mm in area on a PCB, and consist of superior radiation performances. In fact, the proposed CRLH-based antennas are typically five times smaller than conventional, while offering equal or better performance. Furthermore, unlike conventional three-dimensional antennas – which must be designed, tooled and fabricated as a complex metal-and-plastic assembly, the proposed shown in Figs. 8 and 12 are a simple fabricate. This offers manufacturers faster time to market and reduced bills-of-materials due to the simplified design. It also offers a greatly reduced need for fabrication and assembly of antenna components.

In addition, the CRLH-based antenna's ability to concentrate electromagnetic fields and currents near their antenna structures results in achieving better performance.

6. Conclusion

CRLH transmission line metamaterials represent a paradigm shift in electromagnetics engineering and, in particular, for antennas. They exhibit exceptional properties, resulting from their rich dispersion and their fundamental left/right-hand duality. They offer simple and deep insight into metamaterial phenomena, and provide efficient tools for the practical design of components and antennas.
In this paper, the authors introduced a new concept of antenna size reduction based on metamaterial design and printed planar technology, and also presented a novel idea of antenna bandwidth enhancement and radiation's properties improvement based on employing appropriate inductive elements accompanying their optimize values and using low loss materials maximizes radiation efficiency. All simulated results show that the proposed CRLH-based antennas have superior performance and smaller size compared to other conventional antennas design. These antennas have the small size, UWB, lightweight, high gain and efficiency, unidirectional radiation patterns, simple implementation and low cost. The simulated results exhibit that the proposed antennas should be potential candidates to use in the modern wireless communication systems and portable devices.

References

[1] C. Caloz and T. Itoh, *Electromagnetic Metamaterials: Transmission Line Theory and Microwave Applications*. New York: Wiley, 2006.

[2] N. Engheta and R. W. Ziolkowski, *Metamaterials: Physics and Engineering Explorations*. New York: Wiley, 2006.

[3] *FCC First Report and Order on Ultra Wideband Technology*, Feb. 2002.

[4] Y. J. Wang *et al*., "Novel microstrip-monopole integrated ultra-wideband antenna for mobile UWB devices", in *Proc. Radio and Wirel. Conf. RAWCON '03*, Boston, MA, USA, 2003, pp. 87–90.

[5] T. Taniguchi and T. Kobayashi, "An omnidirectional and low-VSWR antenna for the FCC-approved UWB frequency band", in *Proc. IEEE Int. Symp. Anten. and Propag.*, Columbus, OH, USA, 2003, vo1. 3, pp. 460–463.

[6] W. Sorgel, C. Waldschmidt, and W. Wiesbeck, "Transient response of a Vivaldi antenna and a logarithmic periodic dipole array for ultra wideband communication", in *Proc. IEEE Int. Symp. Anten. and Propag.*, Columbus, OH, USA, 2003, vo1. 3, pp. 592–595.

[7] C. J. Lee, M. Achour, and A. Gummalla, "Compact metamaterial high isolation MIMO antenna subsystem", in *Proc. Asia Pacific Microw. Conf. APMC 2008*, Hong Kong, China, 2008, pp. 1–4.

[8] C. J. Lee, A. Gummalla, and M. Achour, "Compact dualband antenna subsystem for MIMO application", in *Proc. Int. Worksh. Antenna Technol.: Small Antenn. Novel Metamater. iWAT 2009*, Santa Monica, CA, USA, 2009, pp. 1–4.

[9] C. Caloz and T. Itoh, *Electromagnetic Metamaterials: Transmission Line Theory and Microwave Applications, The Engineering Approach*. New York: Wiley, 2005.

[10] R. A. Shelby, D. R. Smith, and S. Schultz, "Experimental verification of a negative index of refraction", *Science*, vol. 292, no. 5514, pp. 77–79, 2001.

[11] A. Lai, C. Caloz, and T. Itoh, "Composite right/left-handed transmission line metamaterials", *IEEE Microw. Mag.*, vol. 5, no. 3, pp. 34–50, 2004.

[12] F. J. Herraiz-Martínez, V. González-Posadas, L. E. Garcia-Munoz, and D. Segovia-Vargas, "Multifrequency and dual-mode patch antennas partially filled with left-handed structures", *IEEE Trans. Anten. Propag.*, vol. 56, no. 8, pp. 2527–2539, 2008.

[13] S. G. Mao, S. L. Chen, and C. W. Huang, "Effective electromagnetic parameters of novel distributed left-handed microstrip lines", *IEEE Trans. Microw. Theory Technol.*, vol. 53, no. 4, pp. 1515–1521, 2005.

[14] C. Caloz and T. Itoh, "Novel microwave devices and structures based on the transmission line approach of meta-materials", in *Proc. IEEE MTT-S Int. Microw. Symp. Dig.*, Philadelphia, PA, USA, 2003, pp. 195–198.

[15] Y. M. Pan and S. J. Xu, "A new leaky wave antenna based on channel guide filled with left-hand material for millimeter-wave applications", *Int. J. Infrar. Millim. Waves*, vol. 27, no. 11, pp. 1457–1468, 2006.

[16] A. Sanada, C. Caloz, and T. Itoh, "Zeroth order resonance in the left-handed transmission line", *IEICE Trans. Electron.*, vol. 87-C, no. 1, pp. 1–7, 2004.

[17] W. Huang, N. Xu, V. Pathak, G. Poilasne, and M. Achour, "Composite Right-Left Handed Metamaterial Ultra-Wideband Antenna", in *Proc. Int. Worksh. Anten.a Techno.: Small Anten. Novel Metamater. iWAT 2009*, Santa Monica, CA, USA, 2009, pp. 1–4.

[18] C. Caloz and T. Itoh, *Electromagnetic Metamaterials, Transmission Line Theory and Microwave Applications*. Piscataway: Wiley/IEEE Press, 2005.

[19] N. Engheta and R. W. Ziolkowski, Eds., *Electromagnetic Metamaterials: Physics and Engineering Explorations*. Piscataway: Wiley/IEEE Press, 2006.

[20] C. Caloz and T. Itoh, "Application of the transmission line theory of left-handed (LH) materials to the realization of a microstrip LH transmission line", in *Proc. IEEE In. Symp. Anten. and Propag. Digest*, San Antonio, USA, 2002, pp. 412–415.

[21] A. K. Iyer and G. V. Eleftheriades, "Negative refractive index metamaterials supporting 2-D Waves", in *Proc. IEEE Int. Symp. Microw. Theory Techniq. Digest*, Seattle, USA, 2002, pp. 1067–1070.

[22] C. Caloz and T. Itoh, "Novel microwave devices and structures based on the transmission line approach of metamaterials", in *Proc. IEEE Int. Symp. Microw. Theory Techniq. Digest*, Philadelphia, USA, 2003, pp. 195–198.

[23] R. E. Collin and F. J. Zucker, Eds., *Antenna Theory*, Part 2, Chapters 19 and 20. New York: McGraw Hill, 1969.

[24] G. V. Eleftheriades and K. G. Balmain, *Negative Refraction Metamaterials: Fundamental Principles and Applications*. New York: Wiley, 2005.

[25] C. J. Lee, K. M. H. Leong, and T. Itoh, "Broadband small antenna for portable wireless application", in *Proc. Int. Worksh. Anten. Technol.: Small Anten. Novel Metamater. iWAT 2008*, Chiba, Japan, 2008, pp. 10– 13.

[26] C. J. Lee, K. M. K. H. Leong, and T. Itoh, "Composite right/left-handed transmission line based compact resonant antennas for RF module integration", *IEEE Trans. Anten. Propag.*, vol. 54, no. 8, pp. 2283–2291, 2006.

[27] M. Schussler, J. Freese, and R. Jakoby, "Design of compact planar antenna using LH-transmission lines", in *Proc. IEEE MTT-S Int. Microw. Symp.*, Fort Worth, TX, USA, 2004, pp. 209–212.

[28] E. Weber and F. Nebeker, *The Evolution of Electrical Engineering*, presented at IEEE Press, Piscataway, New Jersey, USA, 1994.

[29] Q. Ye, "Time domain response of ultra-wideband dipole antennas", in *Proc. 2004 Antem/URSI Conf. Anten. Technol. Appl. Electromag.*, Ottawa, Canada, 2004, pp. 661–664.

[30] E. Gazit "Improved design of the Vivaldi antenna", *IEEE Trans. Anten. Propag.*, vol. 135, 1988.

[31] Y. Li, Z. Zhang, J. Zheng and Z. Feng, "Compact heptaband reconfigurable loop antenna for mobile handset", *IEEE Anten. Wirel. Propag. Lett.*, vol. 10, pp. 1162–1165, 2011.

[32] Y. L. Zhao, Y. C. Jiao, G. Zhao, L. Zhang, Y. Song, and Z. B. Wong, "Compact planar monopole UWB antenna with band-notched characteristic", *Microw. Opt. Technol. Lett.*, vol. 50, no. 10, pp. 2656–2658, 2008.

[33] R. Movahedinia and M. N. Azarmanesh, "A novel planar UWB monopole antenna with variable frequency band-notch function based on etched slot-type ELC on the patch", *Microw. Opt. Technol. Lett.*, vol. 52, no. 1, pp. 229–232, 2010.

[34] M. Abdollahvand, G. Dadashzadeh, and D. Mostafa, "Compact dualband-notched printed monopole antenna for UWB application", *IEEE Anten. Wirel. Propag. Lett.*, vol. 9, pp. 1148–1151, 2010.

[35] S. J. Wu, C. H. Kang, K. H. Chen, and J. H. Tarng, "Study of an ultra wideband monopole antenna with a band-notched open-looped resonator", *IEEE Trans. Anten. Propag.*, vol. 58, no. 6, pp. 1890–1897, 2010.

[36] C.-Y. Hong, C.-W. Ling, I.-Y. Tarn, and S.-J. Chung, "Design of a planar ultra wideband antenna with a new band-notch structure", *IEEE Trans. Anten. Propag.*, vol. 55, no. 12, pp. 3391–3397, 2007.

[37] M. Alibakhshi Kenari, "A new compact UWB traveling-wave antenna based on CRLH-TLs for embedded electronic systems", *Int. J. Microw. Wirel. Technol.*, 2014 (in press).

[38] M. Alibakhshi Kenari, "Introducing the new wide band small plate antennas with engraved voids to form new geometries based on CRLH MTM-TLs for wireless applications", *Int. J. Microw. Wirel. Technol.*, 2014 [Online]. Available: http://dx.doi.org/10.1017/S1759078714000099

[39] M. Alibakhshi Kenari, "Printed planar patch antennas based on metamaterial", *Int. J. Elec. Lett.*, 2014 [Online]. Available: http://dx.doi.org/10.1080/21681724.2013.874042

[40] M. Alibakhshi Kenari, "Minimized antenna based on CRLH transmission line for broadband communications", *Int. J. Elec. Lett.*, 2014 (accepted).

Mohammad Alibakhshi-Kenari received his B.S. and M.Sc. degrees in the Electrical Engineering, field of Telecommunication from the Islamic Azad University, Najafabad Branch at Esfahan, Iran on Feb. 2010 and the Islamic Republic of Iran, Shahid Bahonar university of Kerman on Feb. 2013, respectively. His researches interests include microwave and millimeter wave circuits, radars, antennas and wave propagation, composite right/left-handed transmission lines (CRLH-TLs), metamaterial (MTM) applications, integrated RF technologies, embedded systems, electromagnetic waves applications and wireless telecommunication systems. He is now Editor-in-chief in Journal Club for Electronic and Communication Engineering (JCECE) and also works as a reviewer in the several ISI journals such as Elsevier, Taylor & Francis, Wiley, ACES, etc. M. A.-Kenari has served as a Member of the Technical Program Committee (M-TPC) of some of the international conferences such as APACE 2014, APPEIC 2014, MobiWIS 2014, ICEPIT 2014, CICN 2014, ADVCIT 2014, DPNoC 2015, MobiApps 2015, etc. So far, he has been published several papers. His Master Thesis entitled "Designing and Fabricating the Ultra Compact and UWB Antennas based on Metmaterial Transmission Lines with Application in Wireless Radio Transceivers" was approved and granted

by Iran Telecommunication Research Center (ITRC) at Dec. 2012 with grant number of 6987/500/T.
E-mail: makenari@mtu.edu
Faculty of Engineering, Science and Research Branch
Islamic Azad University
Tehran, Iran

Mohammad Naser-Mogaddasi received the B.Sc. degree in Communication Engineering in 1985 from the Leeds Metropolitan University (formerly Leeds Polytechnic), UK. Between 1985 and 1987 he worked as an RF design engineer for the Gigatech company in Newcastle Upon Tyne, UK. From 1987 to 1989, he was awarded a full scholarship by the Leeds educational authority to pursue an M. Phil. He received his Ph.D. in 1993, from the University of Bradford, UK. From 1995, Dr. Naser-Moghadasi joined Islamic Azad University, Science and Research Branch, Iran, where he currently is head of postgraduate studies and also member of Central Commission for Scientific Literacy and Art Societies. His main areas of interest in research are microstrip antenna, microwave passive and active circuits, RF MEMS. Dr. Naser-Moghadasi is member of the Institution of Engineering and Technology, MIET and the Institute of Electronics, Information and Communication Engineers (IEICE). He has so far published over 130 papers in different journals and conferences.

E-mail: mn.moghaddasi@srbiau.ac.ir
Faculty of Engineering, Science and Research Branch
Islamic Azad University
Tehran, Iran